The Shaft of the Type 1 Fimbriae Regulates an External Force to Match the FimH Catch Bond

Johan Zakrisson,[†‡] Krister Wiklund,[†‡] Ove Axner,[†‡] and Magnus Andersson[†‡*]
[†]Department of Physics and [‡]Umeå Centre for Microbial Research (UCMR), Umeå University, Umeå, Sweden

ABSTRACT Type 1 fimbriae mediate adhesion of uropathogenic *Escherichia coli* to host cells. It has been hypothesized that due to their ability to uncoil under exposure to force, fimbriae can reduce fluid shear stress on the adhesin-receptor interaction by which the bacterium adheres to the surface. In this work, we develop a model that describes how the force on the adhesin-receptor interaction of a type 1 fimbria varies as a bacterium is affected by a time-dependent fluid flow mimicking in vivo conditions. The model combines in vivo hydrodynamic conditions with previously assessed biomechanical properties of the fimbriae. Numerical methods are used to solve for the motion and adhesion force under the presence of time-dependent fluid profiles. It is found that a bacterium tethered with a type 1 pilus will experience significantly reduced shear stress for moderate to high flow velocities and that the maximum stress the adhesin will experience is limited to ~120 pN, which is sufficient to activate the conformational change of the FimH adhesin into its stronger state but also lower than the force required for breaking it under rapid loading. Our model thus supports the assumption that the type 1 fimbria shaft and the FimH adhesin-receptor interaction are optimized to each other, and that they give piliated bacteria significant advantages in rapidly changing fluidic environments.

INTRODUCTION

Adhesion of bacteria to cells is commonly mediated via specific adhesin-receptor interactions. In vivo these bacteria are in general exposed to strong shear stress imposed by fluid flows such as expelling of urine, mucosal secretions, blood, and intestinal flows that act as natural defense mechanisms against colonization of pathogenic bacteria. These fluidic flows expose bacteria to drag forces, which sometimes can be considerable, that the bacteria must withstand to not be flushed away. In fact, a bacterium attached to a surface of a host cell can be exposed to severe fluid drag forces with fast time-dependent changes in both magnitude and direction (1–3). For example, in the urinary tract region, the urine flow can reach velocities as high as 1 m/s and be turbulent (4,5).

Uropathogenic *Escherichia coli* are a type of bacteria that express their adhesins on the tip of micrometer-long helical structures called fimbriae or pili (6). It has been shown that these pili are essential for colonization of the urinary tract (7). They have a unique biomechanical behavior with a strongly nonlinear extension-versus-force dependence, and they are thereby believed to play an important role in the attachment of bacteria to host tissue in a fluidic environment (8). Moreover, for type 1 pili, which are expressed predominantly on bacteria in the lower urinary tract and the bladder, it has also been demonstrated that the adhesin-receptor interaction (FimH-mannose) is strongly nonlinear. In fact, by the use of steered molecular dynamics simulations, flow chambers, and force spectroscopy experiments, it has been shown that the FimH adhesin mediates a catch bond, i.e., a bond whose strength is increased by a force (9,10). It is assumed that an advantage of the catch bond, in comparison to the slip bond (for which the lifetime decreases exponentially with the force to which it is exposed), is that it gives bacteria the ability to spread across a target surface under low shear but still adhere strongly under exposure to high shear forces (9); bacteria adhering to a surface by means of catch bonds will show rolling behavior when exposed to low shear but switch to stationary adhesion when exposed to high shear. In addition, it is also assumed that a catch bond is not as amenable to soluble receptorlike inhibitors as is a slip bond.

Since the FimH adhesin is attached to a helical pilus, and both display a nonlinear dependence on force, it is plausible that, as a means to optimize bacterial adhesion under flow (e.g., to optimize the adhesion lifetime under certain conditions), the mechanical properties of the type 1 pilus shaft have coevolved with those of the FimH adhesin (11). To validate this, and to assess to what degree they jointly can reinforce the ability of bacteria to sustain severe fluid drag forces, an improved understanding of the bacterial adhesion process is needed, which in turn requires detailed knowledge about the adhesin, the pili, and the physical interplay of bacteria with their environment.

The shaft of the type 1 pilus, to the tip of which the adhesin is attached, is ~7 nm wide and anchored to the bacterial cell. It is composed of thousands of FimA subunits that are connected in a head-to-tail manner to a chain that coils into an ordered helical arrangement. This complex structure has been investigated in detail by imaging techniques, e.g., transmission electron microscopy and atomic force microscopy, to provide conceptual models of the function in an in vivo situation (12,13). To elucidate the mechanical

Submitted October 26, 2012, and accepted for publication March 29, 2013.

*Correspondence: magnus.andersson@physics.umu.se

Editor: Sean Sun.

0006-3495/13/05/2137/12 $2.00

http://dx.doi.org/10.1016/j.bpj.2013.03.059

properties of the shaft, force spectroscopy measurements using optical tweezers and atomic force microscopes have been carried out on several types of pili, not only type 1 but also P, S, F1C, and type 3 (14–19). It has been found that under exposure to forces equal to or above the so-called uncoiling force, which is the force required to break turn-to-turn interactions in the coil, the shaft can be uncoiled into a linear chain whose length is several times its folded length (20). When the force varies around the uncoiling force, the type 1 pili can also, in a manner similar to that of P pili (14,15), be uncoiled and recoiled a multitude of times without any sign of fatigue. In addition, the uncoiling force has been found to depend on the extension velocity; above the so-called corner velocity, it depends logarithmically on the elongation velocity (18,21). Hence, helixlike pili exhibit dynamic properties (15).

Investigations of the adhesin, the shaft of the pilus, and cell-surface adhesion have been carried out by imaging techniques, force spectroscopy, flow-chamber experiments, and computer simulations (12,16,21–23). However, the amount of work performed that addresses several of these entities jointly, e.g., the physical interplay between adhesin, pili, cell surface, and fluid, is limited. The reason for this has to do with difficulties in relating the mechanical properties at the nano- and microscale to an in vivo situation, i.e., bacterial adhesion to a surface under hydrodynamic interactions from the flow. An example of work that does address these entities jointly is that by Whitfield et al., who, using simulations, examined shear-stabilized rolling of *E. coli* (23). The authors scrutinized the adherence of a cell (modeled as a spherical particle) with protruding filaments of limited flexibility and equipped with catch-bond adhesins to a surface under different shear rates, in a procedure similar to that used in previous flow-chamber experiments. The simulations demonstrated that shear-stabilized rolling can appear as a consequence of an increased number of low-affinity bonds caused by an increased fimbrial deformation (bending) with shear. However, the pili were modeled only as bendable structures; they lacked important biomechanical properties such as uncoiling. In addition, the simulated shear stress was significantly lower than what is expected in certain regions in vivo, in which typical fluid velocities are high and flows are turbulent.

Recently, we presented a general quantitative physical model that elucidates how helixlike biopolymers behave when attached to a spherical cell under exposure to fluid shear (24). In that work, both P and type 1 pili were used as model systems. The sticky-chain model (25), which relates the extension velocity of a pilus to its uncoiling force, was combined with the drag force that acts on a bacterial cell in a fluidic flow. It was found that the uncoiling ability of a pilus, which can give the bacteria a go-with-the-flow ability (24), can reduce significantly the force experienced by the adhesion-receptor bond to levels well below that of the fluid shear force. One of the results from that work is illustrated in Fig. S1 in the Supporting Material, which shows the dependence of the flow on the drag force for a bacterium attached to a surface with a stiff linker (*dash-dotted line*) and a type 1 pilus (*dashed blue line*). It was found that when a bacterium attached with a type 1 pilus is exposed to a fluid flow of 15 mm/s, the drag force to which the adhesin-receptor bond is exposed is reduced by 50% compared to the force measured for a bacterium attached by a stiff linker (or a structure with no elasticity or flexibility) at the same flow velocity. The authors concluded that in the presence of a flow, a type 1 pilus protruding from a sphere can, for a limited amount of time (during the uncoiling process), act as a shock absorber that momentarily dampens an external force, so that the load on the adhesin-receptor bond by which the bacterium adheres to the host cell is significantly reduced (24). That result supports the previous proposed shock-absorber model presented in Forero et al. (11).

Moreover, it was argued that for certain fluid velocities, and at short timescales (a few milliseconds), other types of biopolymers with intrinsic properties similar to those of type 1 pili also can significantly reduce drag forces by uncoiling. It was hypothesized that this type of damping property would be beneficial for bacteria in a fluid environment of turbulent character, where rapid changes in magnitude and direction of flow otherwise could lead to high stress on the adhesin, causing detachment.

However, the fluid conditions in the go-with-the-flow model (24) were the simplest possible. The model is one-dimensional (1D); it considers a bacterium far away from any surface (i.e., it neglects surface effects) that, due to the drag force, moves solely in the direction of the flow. It was also assumed, for simplicity, that the flow was uniform and independent of time. This differs considerably from the conditions to which bacteria are exposed in vivo, which consist of time-dependent and turbulent shear flows. Examples of turbulent fluid environments in vivo can be found in the upper urinary tract, where strong vortices are created from the peristaltic motion, and in the urethra during expulsion of urine. It has been shown that the peristaltic motion can transport boluses at mean flow velocities of up to 30 mm/s (26) and that the contractions in the ureter will induce a flow field that is complex, with both backflows and vortex motion (27,28) causing high variations in shear rates. In addition, in the urethra, the flow can locally reach as high as 1000 mm/s (5), which can transform a laminar flow to turbulent. It is also commonly known that turbulent flows give rise to fluid tsunamis (sweeps and ejections) that can reach into the laminar viscous sublayer and thereby expose bacteria to significantly increased drag forces for milliseconds-long periods (29,30). With these conditions in mind, we developed a model and a simulation procedure to shed light on how piliated bacteria can be affected by such environments during their earliest attachment process. In this work, we thereby present a refined physical model

that simulates attachment of a bacterium to a surface by a FimH adhesin mediated by a type 1 pilus that is exposed to both time-independent and time-dependent shear flows similar to those experienced in vivo.

The work described here thus serves the purpose of elucidating the role of pili uncoiling in the fate of a bacterium attached by a single pilus, in particular, its trajectory in the closest proximity to the attachment point, as well as its adhesion probability (i.e., the survival probability of the FimH adhesin). It is found that the unique extension properties of the shaft significantly reduce the load on the adhesin to a level that corresponds well to the force that previously has been experimentally and theoretically shown to activate the catch bond to give the longest survival probability of the FimH-receptor bond (31), hence correlating some of the key properties of the pilus shaft to those of the adhesin-receptor bond. The work thereby adds support to the assumption that the shaft and the adhesion bond have coevolved during the evolution process.

THEORY AND MODEL SYSTEM

Model system: fluid conditions

Based upon the aforementioned in vivo conditions, for example, the flow in the urethra, the fluid was modeled as a pipe flow with a turbulent core and a thin boundary layer close to the surface (Fig. S2 *A*). The flow in the layer close to the smooth surface, the viscous sublayer, in which the bacteria attach, was assumed to be laminar with a velocity profile increasing linearly from zero at the surface to a maximum value determined by the core flow.

Moreover, in the presence of turbulence, it has been shown that high-velocity flows occasionally sweep down from the core flow into the thin laminar sublayer (Fig. S2 *B*) (2,29). These sweeps are created by strong vortices outside the viscous sublayer, temporarily increasing the shear rate near the surface (32). The effect of these temporary sweeps was modeled by momentarily changing the shear rate of the velocity profile in the viscous sublayer (Fig. S2, *A* and *B*).

A nominal shear rate, S_0, was defined, chosen to correspond to a reference flow velocity of 8 mm/s at a distance of 3 μm above the surface, which represents a shear rate of ~2700 s^{-1}. This reference velocity was estimated by considering the general flow in a urethra, i.e., a 5-mm-diameter pipe with a center velocity of 1000 mm/s; the laminar sublayer close to the surface was modeled in a standard fashion using a linear velocity profile determined by the pipe-wall shear stress (30).

To mimic flows and their changes in our model, simulations were made at three different shear rates, S_1, S_2, and S_3, representing values of S_0, $2S_0$, and $3S_0$, respectively, where the latter two rates predominantly represent an increased rate during a momentary sweep. A transient increase of the flow implies a sudden increase of the drag force adding tensile stress to the pilus and thereby to the adhesin.

Model system: tethered bacterium exposed to fluid flow

Fig. 1 displays a schematic illustration of the model presented in this work. A bacterium is attached to a surface by a pilus and exposed to a linear flow profile. The model takes into account four important conditions: 1), a two-dimensional (2D) motion of bacteria relative to the surface; 2), time-dependent fluid velocity shear profiles; 3), drag-force corrections for near-surface motion, both parallel (33) and perpendicular motion (34); and 4), the allosteric catch-bond properties of the FimH adhesin and the mechanical properties of the shaft.

Pili uncoiling under 1D conditions

The model developed here is based in part on our previous 1D model for damping of the adhesion force of a bacterium attached by a single pilus exposed to a flow (24). That work describes a bacterium modeled as a rigid sphere in a uniform

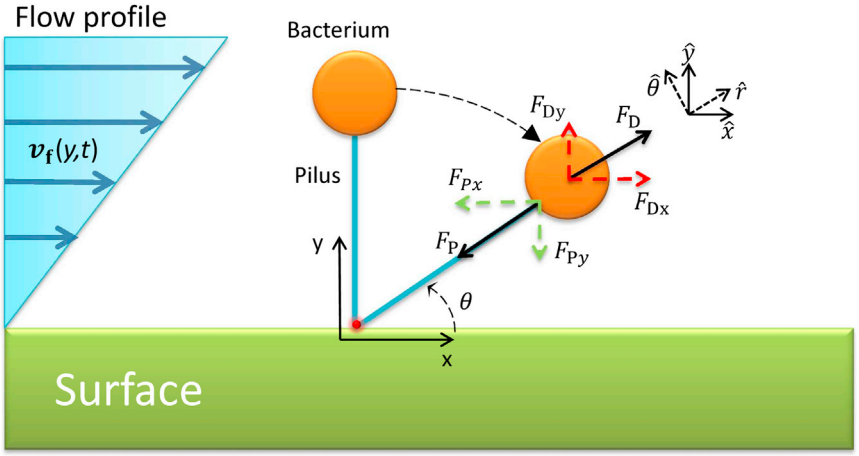

FIGURE 1 Symbolic representation of the nomenclature used in the model. The red point represents both the origin of the coordinate system and the position at which the adhesin adheres to a surface receptor. All entities displayed in the figure (θ, F_P, F_{P_x}, F_D, etc.) generally take positive values and are described in detail in the text.

flow attached to a surface by a pilus of length L. The sphere was constrained to move in one dimension, parallel to the flow, exposed to a Stokes drag force given by

$$F_{\mathrm{D}} = 6\pi\eta r\left(v_{\mathrm{f}} - v_{\mathrm{b}}\right), \tag{1}$$

where η is the dynamic viscosity of the fluid, r is the radius of the sphere, and v_{f} and v_{b} are the fluid velocity and the velocity of the bacterium with respect to the surface. The sphere was assumed to be neutrally buoyant and to follow the flow when it suddenly was attached by a pilus (alternatively, when it suddenly was exposed to a flow). Since the sphere is anchored by an extendable pilus, its velocity is equal to the elongation velocity of the pilus, i.e., $v_{\mathrm{b}} = \dot{L}$, which in turn is related to the tensile force to which the pilus is exposed (which is equal to that applied to the sphere as well as that experienced by the adhesin), F_{P}, which can be written as (see Zakrisson et al. (24) for a detailed derivation)

$$\dot{L}(F_{\mathrm{P}}) = \dot{L}^{*} e^{(F_{\mathrm{P}} - F_{\mathrm{SS}})\Delta x_{\mathrm{AT}}\beta}\left[1 - e^{-(F_{\mathrm{P}} - F_{\mathrm{SS}})\Delta x_{\mathrm{AB}}\beta}\right], \tag{2}$$

where $\dot{L}^{*}$ is the corner velocity for the uncoiling of the pilus, F_{SS} is the steady-state uncoiling force, Δx_{AT} is the turn-to-turn bond length from the ground state to the transition state, $\beta = 1/kT$, where k is Boltzmann's constant and T is the temperature, and $\Delta x_{\mathrm{AB}} = \Delta x_{\mathrm{AT}} + \Delta x_{\mathrm{TB}}$, where Δx_{TB} is the distance from the transition state to the open state. Due to the low mass of the bacterium, the effect of inertia was neglected, since it gives rise to forces several magnitudes lower than the fluid forces. Moreover, since the model was 1D, F_{P} was at every instance considered equal to F_{D}. This model demonstrated that the force to which an adhesin is exposed can be significantly reduced due to the elongation properties of the pilus; as long as the pilus is extending, the force acting on the adhesin is lower (often significantly lower) than that of a stiff linker (for which the force is given by Eq. 1, with $v_b = 0$). Although this 1D model can illustrate the ability of the pilus to dampen the drag force, it cannot provide a full picture of the adhesion phenomena of a bacterium in a flow. In particular, it does not take the shear profile and near-surface effects into account. To address these effects requires a 2D model.

2D movement of a bacterium attached by a pilus under a linear shear profile

In our refined model, presented here, a tethered bacterium (again modeled as a sphere) is allowed to move in two dimensions in a fluid with a linear shear profile, i.e., with $\mathbf{v}_{\mathrm{f}}(y) = Sy\hat{\mathbf{x}}$, where S is the shear rate, y is the distance from the surface (measured in the direction normal to the surface), and $\hat{\mathbf{x}}$ is the unit vector parallel to the surface (see Fig. 1). Since a bacterium attached to the surface by a pilus and exposed to a force will move in the flow, it will in general have a position-dependent velocity that can be expressed as

$$\mathbf{v}_{\mathrm{b}}(y) = v_{\mathrm{bx}}(y)\hat{\mathbf{x}} + v_{\mathrm{by}}(y)\hat{\mathbf{y}}, \tag{3}$$

where $v_{\mathrm{bx}}(y)$ and $v_{\mathrm{by}}(y)$ are the components of the velocity in the $\hat{\mathbf{x}}$- and $\hat{\mathbf{y}}$-directions, respectively, and where $\hat{\boldsymbol{y}}$ is the unit vector perpendicular to the surface (see Fig. 1). Note that whereas $v_{\mathrm{bx}}(y)$ is positive, $v_{\mathrm{by}}(y)$ takes a negative value as the bacterium approaches the surface. In addition, the model also allows for the influence of sweeps by allowing the shear rate to be time-dependent, i.e., $S(t)$. By assuming that y describes the position of the sphere, which in turn is time-dependent, the bacterium will experience a flow velocity, $\mathbf{v}_{\mathrm{f}}$, that depends on both its position, $y(t)$, and time, i.e.,

$$\mathbf{v}_{\mathrm{f}}[y(t), t] = S(t)y(t)\hat{\mathbf{x}}. \tag{4}$$

Hence, the fluid model not only takes into account the altered flow velocity experienced by the sphere as it moves in the fluid, it also depicts the influence of a change in flow velocity on the sphere (due to a time-dependent shear rate).

A bacterium exposed to a flow will be affected by several forces, of which the two dominant forces are the pilus force, $\mathbf{F_P}$, which has a magnitude of F_P and is directed along the direction of the pilus, here denoted by $\hat{\boldsymbol{r}}$, and the fluid drag force, $\mathbf{F_D}$, originating from the relative motion of the bacterium with respect to the fluid (Fig. 1). These two forces can be written, conveniently, in terms of their x- and y-components as

$$\mathbf{F}_{\mathrm{P}}(t) = F_{\mathrm{P}}(t)\hat{\mathbf{r}} = F_{\mathrm{Px}}(t)\hat{\mathbf{x}} + F_{\mathrm{Py}}(t)\hat{\mathbf{y}} \tag{5}$$

and

$$\mathbf{F}_{\mathrm{D}}(t) = F_{\mathrm{Dx}}(t)\hat{\mathbf{x}} + F_{\mathrm{Dy}}(t)\hat{\mathbf{y}}. \tag{6}$$

Lift forces arising from shear flow (35,36) and from the presence of a wall (37) can be neglected, since these are insignificant compared to the other forces. As for our 1D model (24), the sphere is assumed to be neutrally buoyant over the timescale studied.

As discussed in Zakrisson et al. (24), the drag force experienced by the sphere will depend on the relative motion of the bacterium with respect to the velocity of the fluid. However, since the sphere is close to a wall, proximity effects need to be taken into account. This is normally done by modifying the Stokes drag force by the use of a correction term. However, since the motion of the sphere has components in both the parallel and perpendicular directions with respect to the surface, and the effect of the presence of the wall is dissimilar in the two directions, it is appropriate to write (34,38)

$$F_{\mathrm{Dx}}[y(t), t] = C_{\mathrm{x}}[y(t)]6\pi\eta r[S(t)y(t) - v_{\mathrm{bx}}(t)] \tag{7}$$

and

$$F_{\mathrm{Dy}}[y(t), t] = -C_{\mathrm{y}}[y(t)]6\pi\eta r v_{\mathrm{by}}(t), \tag{8}$$

where $C_x[y(t)]$ and $C_y[y(t)]$ are corrections to the Stokes drag force experienced by a bacterium close to a wall moving in the x- and y-directions, respectively. For motions parallel to the surface, we use the fifth-order correction factor derived by Faxen, as given, e.g., by Eq. 7-4.28 in Happel and Brenner (34), which reads

$$C_x[y(t)] = \left\{1 - \frac{9}{16}\left[\frac{r}{y(t)}\right] + \frac{1}{8}\left[\frac{r}{y(t)}\right]^3 - \frac{45}{256}\left[\frac{r}{y(t)}\right]^4 - \frac{1}{16}\left[\frac{r}{y(t)}\right]^5\right\}^{-1}, \quad (9)$$

where r is the radius of the bacterium and y is the distance from the surface to the center of the bacterium. To correct for the motion perpendicular to the surface, we use the approximated correction factor that is valid for $y/r>1.1$, which can be written as (39)

$$C_y[y(t)] = \left\{1 - \frac{9}{8}\left[\frac{r}{y(t)}\right] + \frac{1}{2}\left[\frac{r}{y(t)}\right]^3 - \frac{57}{100}\left[\frac{r}{y(t)}\right]^4 + \frac{1}{5}\left[\frac{r}{y(t)}\right]^5 + \frac{7}{200}\left[\frac{r}{y(t)}\right]^{11} - \frac{1}{25}\left[\frac{r}{y(t)}\right]^{12}\right\}^{-1}. \quad (10)$$

Since the effect of inertia can be neglected, force balance must prevail at every moment. This implies that

$$F_{Dx}[y(t),t] = F_{Px}[y(t),t] = F_P[y(t),t]\cos[\theta(t)] \quad (11)$$

and

$$F_{Dy}[y(t),t] = F_{Py}[y(t),t] = F_P[y(t),t]\sin[\theta(t)], \quad (12)$$

where $\theta(t)$ is the angle of the pilus with respect to the surface, as indicated in Fig. 1.

These equations need to be solved for the position and velocity of the sphere, as well as the drag and pilus forces, under the condition that the movement of the sphere is constrained by a tether behaving as a pilus, according to the model given above (see Eq. 2). However, the coupling of the position and velocity of the sphere to the instantaneous drag and pilus forces (i.e., Eqs. 7–12), as well as coupling of the pilus force to the elongation velocity of the pilus (Eq. 2), makes the system difficult to solve by analytical means. In short, they imply that as the sphere is exposed to a flow and moves toward the surface, it will experience a position-dependent velocity and be exposed to a position-dependent drag force (both of which are also time-dependent in the presence of sweeps), which in turn give rise to a varying force to which the pilus is exposed. Thus, as described in some detail in the Supporting Material, the set of equations given above have been solved by numerical means.

As discussed in some detail below, and as schematically illustrated in Fig. 2, this system of equations indicates that the sphere will move in curved trajectories. For low flows (and thereby low drag forces), the pilus will not uncoil, and thus its length, L, will not change, being equal to its original coiled length, L_0. The sphere will then be constrained into a circular motion controlled by a pilus with a fixed length, L_0 (Fig. 2, *dashed arrow*).

For high enough flows, however, the force acting on the pilus will induce uncoiling (and possibly also subsequent recoiling), which gives rise to an extension (and a possible contraction) of the pilus, i.e., a time-dependent length, $L(t)$, whose elongation velocity at each moment in time is given by Eq. 2. As further discussed in the Supporting Material, the part of the bacterium velocity due to unfolding will be in the direction of the external force, i.e., in the $\hat{\mathbf{x}}$-direction. This not only will affect the motion trajectory of the bacterium (Fig. 2, *solid curved arrows*) but also will decrease the force the adhesin experiences in a manner similar to that of the 1D model described in Zakrisson et al. (24).

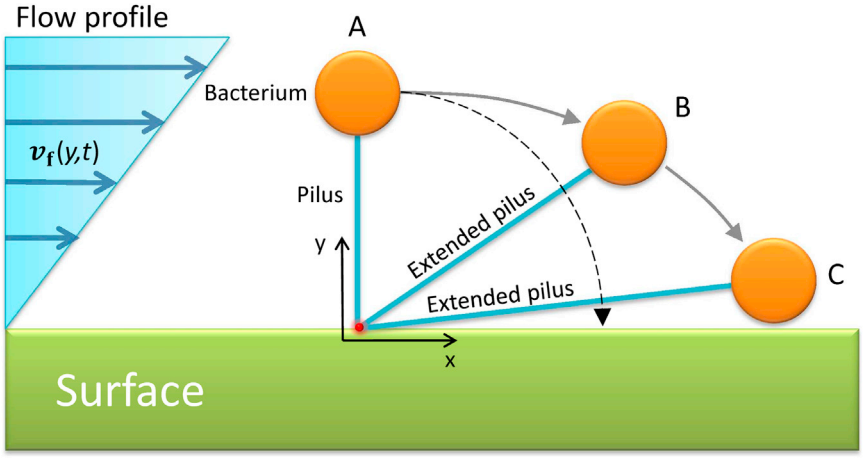

FIGURE 2 The trajectory of a bacterium tethered to a surface with a stiff linker (*black dashed arrow*) and an extendable pilus that elongates by uncoiling when the shear force is higher than the uncoiling force (*gray solid arrows*).

To investigate the influence of the extendability of the pilus on the model system—in particular, the movement of the bacterium, the force acting on the adhesin, and the survival probability of the bacterium—two types of tethers that constrain the motion of the sphere were considered, a stiff linker and an extendable pilus with biomechanical properties of the type 1 pilus. The motion of a bacterium attached by a stiff linker is therefore used as the reference system to which we compare the biomechanical properties of an extendable pilus with dynamic properties.

The FimH-mannose bond

The type 1 pilus adhesin, FimH, is expressed at the tip of the pilus. It anchors the bacteria to receptors (mannose) on the surface of the host and hence mediates the forces that act on the bacterium. The FimH-mannose bond has been modeled successfully by an allosteric catch-bond model that can predict the lifetime of a bond capable of switching between three different states, a weak, a strong, and an unbound state (22). The model describes the motion of *E. coli* bacteria rolling on mannose-bovine serum albumin and predicts the force spectroscopy data performed by constant-velocity atomic force microscopy (22,31).

The probability as a function of time of the FimH-mannose bond to reside in state i, B_i, where $i = 1$ and $i = 2$ represent the weak and strong bound states, respectively, can be described by two differential equations (22):

$$\frac{dB_1(t)}{dt} = -\{k_{10}[F(t)] + k_{12}[F(t)]\}B_1(t) + k_{21}[F(t)]B_2(t) \tag{13}$$

and

$$\frac{dB_2(t)}{dt} = k_{12}[F(t)]B_1(t) - \{k_{20}[F(t)] + k_{21}[F(t)]\}B_2(t), \tag{14}$$

where k_{10}, k_{20}, k_{12}, and k_{21} represent state transition rate coefficients, with an exponential dependence on force, described by the Bell equation, $k_{ij}[F(t)] = k_{ij}^o \exp[F(t) \times x_{ij}/kT]$, where k_{ij}^o is the thermal rate constant, F represents the applied force, x_{ij} is the distance to the transition state, and kT is the thermal energy (40). These two equations determine the survival probability of the FimH-mannose bond, B_1 and B_2, as a function of time after bond formation for a given force.

In our simulation of the full fluid-bacteria-pilus-FimH system, described by Eqs. 2, 7, 8, 13, and 14, we used transition-rate parameter values originating from Yakovenko et al. (31), listed in Table S1. As described in some detail in the Supporting Material, the force responses of the two tethers, stiff linker and extendable pilus, were determined first, by solving Eqs. 2, 7, and 8. The time-dependent force data from such simulations were then used to assess the survival probability of the FimH-mannose bond as a function of time by solving Eqs. 13 and 14.

RESULTS

Trajectory for an attached bacterium and the force experienced by the adhesin in a steady flow

To investigate the 2D movement trajectory of a bacterial cell during attachment to a surface exposed to different flow conditions, three shear rates, S_1–S_3, were considered in the simulations. The bacterium was assumed to have an effective radius of 1.0 μm and to be equipped with a single 2-μm-long tether. It was initially positioned ($t = 0$) directly above the anchoring point (i.e., at $x = 0$, $y = 3$ μm). The flow exposed the bacterium to a drag force (given by Eqs. 7 and 8) that sets the bacterium into motion.

The tether was first given properties of a stiff linker, for all shear rates, (i.e., with no elasticity). For this case, the cell moved along a circular trajectory (Fig. 3 *A*, *solid black line*). As alluded to in the Supporting Material, the simulations were terminated when the membrane of the bacterium was at a distance 0.2 μm above the surface (the simulation termination distance, STD). This was caused by the fact that the Stokes drag-force correction coefficients are not valid for distances close to the surface.

The stiff linker was then replaced with an extendable pilus (with biomechanical properties given by those of type 1 pili). Since its elongation velocity, modeled by Eq. 2, depends on the drag force, it is directly related to the shear rate and thereby varies with position above the surface. At high shear rates, the drag force applies sufficient tension to the pilus to uncoil it. Based on previous experimental findings, it was assumed that the uncoiling commences at a force of 30 pN (16). For the case with the lowest shear rate, S_1 (Fig. 3 *A*, *green dashed line*), this force is obtained at a position of ~2 μm, after which the bacterium takes a slightly shallower path in comparison to the simulation with the stiff linker.

For the two higher shear rates, S_2 and S_3, the trajectories become significantly elongated, coinciding at first with that of the stiff linker until the tensile force reaches the threshold value for uncoiling. In the case with a shear rate of S_2 (Fig. 3 *A*, *blue dash-dotted curve*), the bacterium is translated to a position 11 μm from the tether point before it reaches the STD. Movie S1 shows the movement of the bacterium at a shear rate of S_2 (for both a stiff linker and a type 1 pilus). For the case with a shear flow of S_3 (Fig. 3 *A*, *red short-dashed curve*), the bacterium uncoils completely before it reaches the STD, which it does at a position 14 μm from the tether point. From this position, it acts as a stiff linker.

Fig. 3 *B* shows the corresponding force acting on the pilus (thereby also on the adhesin-receptor bond at the anchor point) as a function of time during the trajectories explored

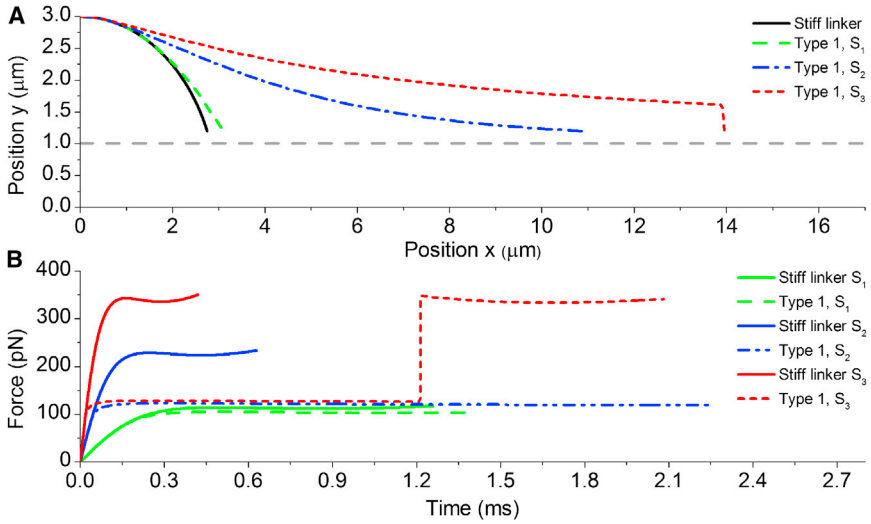

FIGURE 3 (*A*) Trajectory of a bacterium tethered with either a stiff linker (*solid black curve*) or a type 1 pilus (*dashed curves*) exposed to different flows, S_1, S_2, and S_3. The bacterium modeled has an effective radius of 1.0 μm and the length of the tether is 2 μm. The position given represents the center position of the bacterium. The gray dashed horizontal line therefore represents the position at which the bacterium touches the surface. (*B*) The force experienced by the adhesin in the various cases.

by the bacterium in Fig. 3 *A*. As above, the solid curves represent the stiff linker and the various dashed curves correspond to the type 1 pilus, both types exposed to the three different shear rates; the green, blue, and red curves correspond to shear rates of S_1, S_2, and S_3, respectively. The data show that even though the trajectories for the bacterium tethered with a stiff linker (*solid curves*) are identical for all shear rates (Fig. 3 *A*, *black solid curve*), the forces on the anchor point differ significantly. The peak forces for the stiff linker exposed to the three shear rates are ~100, ~225, and ~350 pN, respectively.

At the lowest shear force, S_1, the type 1 pilus shows a response similar to that of the stiff linker (Fig. 3 *B*, *green curves*), experiencing only a low uncoiling velocity. The simulations indicate that for the higher shear rates, the elongation properties of the pilus give rise to a significant reduction of the peak force. For both the S_2 and S_3 shear rates (Fig. 3 *B*, *blue and red dashed curves*, respectively), the force is reduced to ~120 pN, which is lower by a factor of 2 and 3, respectively, than in the case where the bacterium is attached by a stiff linker. In addition, the red curve shows that for the highest shear rate, S_3, the force eventually increases from 120 pN to 350 pN at ~1.2 ms. This sudden increase in force originates from the pilus having fully uncoiled, at which point it acts as a stiff linker.

Trajectory for an attached bacterium and the force experienced by the adhesin in a transient flow

The fluid dynamics of the urinary tract system is complex, with peristaltic activities as well as high fluid-flow velocities leading to turbulence. Turbulence in turn gives rise to transient sweeps and ejections that instantaneously change the fluid profile in the viscous sublayer. To better understand how turbulence can affect a tethered bacterium, sweeps were simulated by adding a transient increase of the shear flow at given onset times of 0, 0.25, 0.5, 0.75, and 1 ms.

Fig. 4, *A* and *B*, shows simulations of sweeps (modeled as step increases in the shear rate from S_1 to S_2 and from S_1 to S_3, respectively) that appear at different onset times. As shown by the solid curve in Fig. 4 *A*, for a bacterium attached with a stiff linker, the trajectories are again identical (they all overlap). For an extendable pilus exposed to a sudden sweep with a shear rate of S_2, the total translation length decreases significantly (from 11 to 4.5 μm) as the onset of the sweep is increased (from 0 to 1 ms). This comes from the fact that for the late-onset times, the bacterium is exposed to a force above the uncoiling force for only a fraction of its trajectory. Hence, it reaches the STD mainly coiled. As illustrated in Fig. 4 *B*, for the largest shear rate, S_3, the pilus reaches full elongation (14 μm) for all onset times up to 0.5 ms.

The force acting on the anchor point as a function of time for three of the above-mentioned cases with sudden onset of sweeps with S_2 and S_3 shear rates is shown in Fig. 5, *A* and *B*, respectively. The solid curves show the force acting on the anchor point for a stiff linker, with different onset times. The red solid curve corresponds to an onset time of 0 ms, whereas the green and blue curves represent onset times of 0.5 and 1 ms, respectively. The simulations show that the onset of the sweep instantaneously increases the force. For the lower sweep shear rate, S_2, the force increases from 100 to ~225 pN (Fig. 5 *A*, *green and blue solid curves*), whereas for the highest sweep shear rate, S_3, it increases to ~350 pN (Fig. 5 *B*, *green and blue solid curves*).

The dashed curves in Fig. 5 represent a bacterium attaching by a type 1 pilus under the same conditions applied for the stiff linker. Fig. 5 *A* shows data from the simulations with shear rate S_2, where the uncoiling capability of the type 1 pilus reduces the force on the adhesin (relative to that on the stiff linker) from ~225 to ~120 pN irrespective of the onset time of the sweep. For the case with the higher sweep shear rate, S_3 (Fig. 5 *B*), the force is reduced to the same level as with S_2, as long as the pilus uncoils. The steep

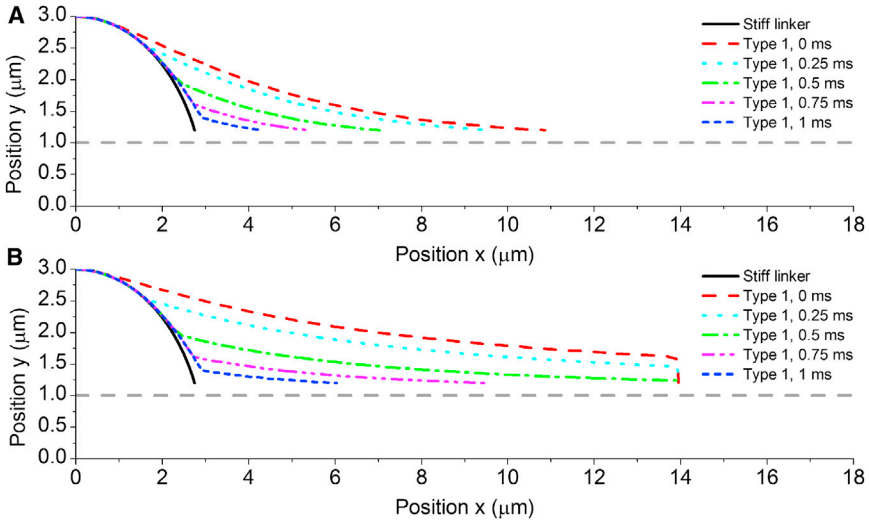

FIGURE 4 Trajectory of a bacterium exposed to five different transient sweeps. The solid black curves correspond to a bacterium attached by a stiff linker, whereas the dashed curves represent the trajectories for the bacterium attached with a type 1 pilus. In all cases, at time 0 the bacterium was exposed to a flow profile with the nominal shear rate of S_0 (corresponding to a linear shear with a flow velocity of 8 mm/s 3 μm above the surface). The sudden sweeps increase the shear rate at given times after the start of the simulation, as indicated in the key. (*A*) The shear rate was increased by a sweep from S_0 to S_2. (*B*) The shear rate was increased by a sweep from S_0 to S_3.

increases in force to ~350 pN at 1.2 and 2.1 ms for the cases with 0- and 0.5-ms onset time (Fig. 5 *B*, *red and green dashed curves*, respectively) originate from the fact that the pilus has been fully uncoiled, in which state it acts as a stiff linker.

The influence of pilus uncoiling and bacterial trajectory on the survival probability of the FimH adhesin

The results presented above describe how the force acting on the anchor point (and thereby the adhesin-receptor bond) is affected by the properties of the tether and the fluid conditions. To get a better understanding of how these forces affect the lifetime of the adhesin-receptor bond, and thereby the bacterial adhesion lifetime, the model was extended to also include the catch-bond properties of the FimH adhesin (9). The adhesin was modeled as an allosteric catch bond described by Eqs. 13 and 14, with the four force-dependent kinetic coefficients used in Yakovenko et al. (31). In that work, the lifetime of the FimH-mannose bond was investigated for a constant loading rate (i.e., a linearly increasing force with time). In our case, we couple the FimH-mannose bond model to the actual time-dependent force to which the adhesion-receptor bond is exposed under the attachment process simulated above. As the flow exposes the bacterium to a drag force, the tension on the tether changes the force on the adhesin, which in turn modulates the probability of staying bound.

To verify our numerical simulations of the FimH-mannose-bond model, we solved Eqs. 13 and 14 for the three loading rates considered by Yakovenko et al. (31). Our findings are in agreement with the results of that study (31), confirming the numerical procedure used for solving these equations.

The probability of a bacterium staying attached is given by the survival-probability distribution of the adhesion-receptor bond. Fig. 6 shows the probability distribution for

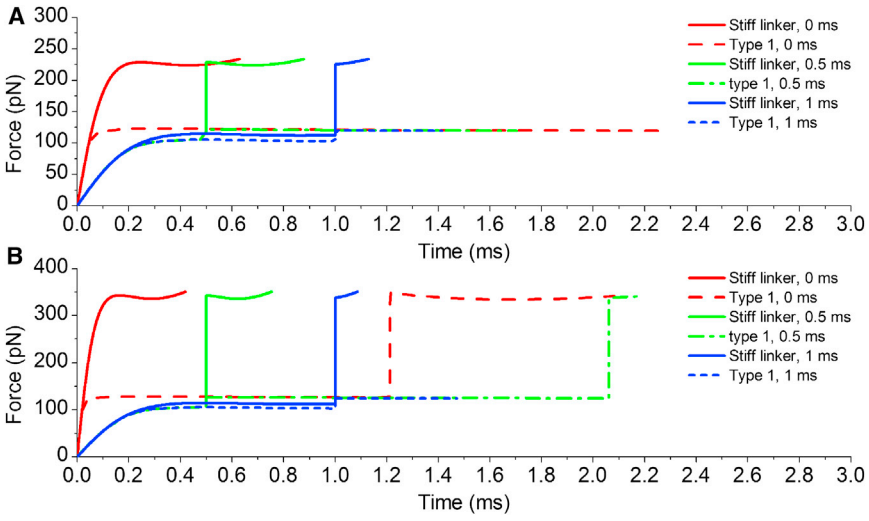

FIGURE 5 Force experienced by the adhesin for three of the flow conditions considered in Fig. 4 (when the transient sweep increases the shear rate at 0, 0.5, and 1 ms after the start of the simulation). The denotations of the various curves are indicated in the key, and the shear sweeps for *A* and *B* are as in Fig. 4.

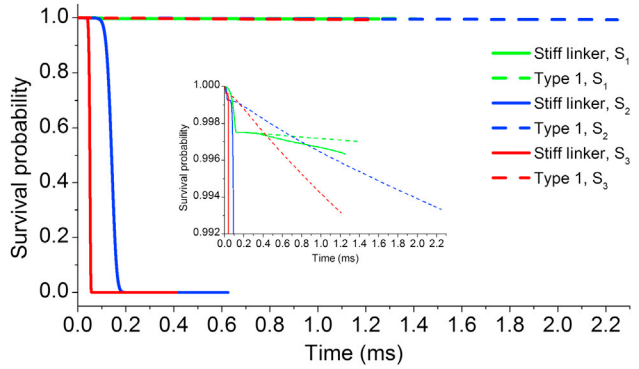

FIGURE 6 Survival probability for a FimH-mannose bond when the bacterium is tethered via a stiff linker (*solid curves*) or a type 1 pilus (*dashed curves*) and exposed to three different shear rates, S_1, S_2, and S_3. The figure shows that for the stiff linker, the survival probability rapidly decreases toward zero in <0.2 ms, whereas for the type 1 pilus it remains close to 1 for a considerable time. (*Inset*) Decrease in the survival probability of the bacteria attached by the two types of tether. After 1.2 ms at S_3, the pilus is fully uncoiled (*red dashed curve*), i.e., the survival probability will rapidly go toward zero (not explicitly shown). The plateau represents the period after the catch bond changes conformation state from the weak to the strong binding configuration.

a stiff linker and a type 1 pilus (*solid and dashed curves*, respectively) for shear rate S_2, which correspond to the blue curves in Fig. 3 *B* that initially increase linearly and thereafter flatten out. The figure shows that for a bacterium attached by a stiff linker, the survival probability drops drastically (to values close to zero) after a short time (<0.2 ms). For a bacterium adhering with a type 1 pilus, on the other hand, it remains high (>0.99) through the entire simulation (until the bacterium reaches the STD). In addition, early in the simulation (at ~0.05 ms), the time development of the survival probability for both linkers changes to a plateaulike dependence. This is attributed to the fact that the bond alters conformation state, from the weak to the strong binding configuration, for which the lifetime is long for the pertinent force.

Survival-probability distributions for a variety of transient flows were also simulated. Fig. 6 shows such distributions for the six cases displayed in Fig. 3 *B*. Although not explicitly shown here, it was found that the situations presented in Fig. 5, representing delayed onsets of sweep (Fig. 5, *A* and *B*, *green and blue curves*, respectively), gave rise to survival-probability distributions that are similar in form to those shown in Fig. 6, mainly shifted in time. The survival-probability distributions presented in Fig. 6 can therefore be seen as typical for a broad variety of situations.

Influence of the parallel and normal drag correction coefficients on a tethered bacterium under flow

In addition to the above results, we also investigated the impact of the normal and parallel drag correction coefficients (Eqs. 9 and 10) in the simulations. Using the S_2 shear rate under the same conditions as presented in Fig. 4 *B*, four situations were compared, with and without each of the two correction coefficients. The results presented in Fig. S5 show the force on the adhesin for the stiff linker and the type 1 pilus (*solid and dashed curves*, respectively) with and without each drag coefficient. For the stiff linker, using the model described in this work, which incorporates both correction coefficients, the maximum force was found to be ~225 pN. For the two cases where only one of the two coefficients was included, either the normal or the parallel, the maximum force was found to be ~190 pN. For the uncorrected case, it became ~125 pN. Thus, it was concluded that for a stiff tether, if the correction coefficients are not used, the simulations underestimate the force by almost 50%. For the case with the type 1 pilus, the influence of the correction coefficients on the maximum force is significantly smaller; the maximum forces were found to be ~120 pN for all four cases. The reason for this is the force-damping ability of the pilus, which disguises the effect of the correction coefficients. However, the time evolution of the motion, and thereby also of the force exposure, are affected by these. The simulations predict that when the correction coefficients are included, it takes five times as long to reach STD as when they are not included.

DISCUSSION AND CONCLUSION

It is nontrivial to scrutinize experimentally the initial attachment or the adhesion process of a bacterium to a surface under different fluidic conditions. However, it is possible to characterize separate parts of the otherwise complicated cell-surface adhesion process, i.e., the receptor-ligand interaction, various properties of the pili, and the fluid-cell shear force. Receptor-ligand interactions and the biomechanical properties of a pilus can be assessed in great detail by force spectroscopic investigations in which entities such as bond lengths, bond energies, and transition rates can be assessed. These experiments do not, however, give any information about how the fluid gives rise to a shear force that acts on a tethered cell. Complementary techniques, e.g., parallel-plate flow-chamber instrumentation can provide information about how the drag force of a fluid interacts with a cell under various conditions, e.g., when the cell is moving freely with the fluid, rolling on a surface, or staying bound, for different fluid flow velocities. However, such a technique cannot be used to scrutinize how pili interact with a surface or to assess the number of pili by which a bacterium binds at each moment. Nor is it trivial to experimentally assess how intrinsic mechanical properties, such as the pilus uncoiling force and bond transition rates, affect the motion of a cell in a flow and the associated force experienced by the adhesin-receptor bond. When a complex combined phenomenon is difficult to assess experimentally, computer simulations,

based on appropriate models and input parameters, can be a powerful complement.

We present in this work a model that describes the effects of force on the adhesin-receptor bond of a type 1 pilus by which an *E. coli* binds to a surface, and the extent to which the bacterium can remain bound to the surface when it is exposed to a time-dependent fluid flow. Our work is based upon models for cell-fluid interactions, pilus uncoiling, and the allosteric FimH catch bond that previously have shown good agreement with experimental data (22,23,39,41). It makes use of input parameters that have been assessed by force spectroscopy and flow-chamber experiments. The model is investigated and assessed by simulations.

These simulations allowed us to follow in detail the 2D trajectory of a tethered bacterium and the load on the adhesin-receptor bond during translation. It is found that pilus uncoiling allows the bacterium to translate significant distances (~10–14 μm) in the direction of the flow while still being attached to a receptor under sustainable tension. This allows an attached bacterium to drift close to the surface, where it is exposed to lower drag forces, which can increase the probability of additional pili attaching. As previously shown both experimentally and by simulation, the latter can result in shear-stabilized rolling, i.e., enhanced adhesion due to the fluid forces. For example, in simulations aimed at describing the shear-stabilized rolling behavior of *E. coli*, even though pili were simulated without uncoiling ability and the shear rates were significantly smaller than in our work, it was found that shear stress can give rise to compressive forces on the fimbriae that result in fimbrial deformation (23). Fimbrial deformation allows short pili to attach to the surface also, increasing the adhesion lifetime of a bacterium. Our simulations (providing 15–20 pN at S_2) support the previous findings (23) that the force pushing the cell toward the surface is sufficiently high to bend and compress type 1 fimbriae.

Our approach of calculating the drag force as a function of the position of the bacterium relative to the surface, at the same time incorporating the unique biomechanical properties of type 1 pili, has allowed us to estimate the survival probability of the FimH adhesin-receptor bond under dynamic flow conditions. Since the survival probability of a bond is directly related to the force to which it is exposed, our approach provides information as to how the bacterial adhesion time is influenced by phenomena such as pilus uncoiling. It was found by the simulations that the maximum force experienced by the adhesin is strongly regulated by pilus uncoiling. For example, for a shear rate of S_2, the maximum force mediated by a stiff linker, ~220 pN, was reduced to ~120 pN when mediated by a type 1 pilus.

A previous study showed that for the most effective binding of the FimH adhesin, the force should be sufficient to fast enough activate the conformational change of the FimH adhesin into its stronger bound state, here designated the critical force (31). For low forces, the bond remains in the weakly bound state and therefore has a short survival probability. The force should not, however, be increased substantially above the critical force, since this could overpower the bond. Once the bond has switched to its stronger conformation it will remain there for a wide range of forces (31). Hence, a structure that can modulate the force on the adhesin so that it rapidly reaches the critical force, and thereafter keeps it at a sustainable level, provides the longest bond lifetime. Our work shows that even if the bacteria are exposed to very high flows, the shaft of the type 1 pilus can reduce the force to a value similar to that of the critical force of the FimH (~100 pN) and thereby prolong the adhesion lifetime. The survival probability of bacteria attaching by a type 1 pilus can therefore remain high ($>$0.99) over a significant time. In addition, simulations concerned with various sweep-onset delays (whose responses are similar to that displayed in Fig. 6 but are not explicitly shown) indicate that short sweeps do not have to be devastating for bacterial adhesion; the extensibility of pili can regulate the force during temporary sweeps to a sustainable level. This implies that a bacterium can benefit from a large survival probability even under short but intense sweeps (as long as the pili can uncoil). This implies that the bacterium can stay bound to a surface for a long time even if it is exposed to a significant fluid drag force. This finding may explain why some bacteria can withstand the natural defense mechanisms of urine in vivo or the peristaltic transport of the lumen.

Many works dealing with adhesive experiments and simulations in flows neglect the influence of the correction coefficients for near-surface motion. We show here that the influence of these on the drag forces, as well as the time to reach the surface, is of importance for a cell tethered to a surface with a stiff linker. Both the drag forces and the times were significantly different when the coefficients were included from when they were not. However, the differences were found to be less significant for the type 1 pilus. For a stiff linker, the simulated forces differ by ~50%, whereas for the type 1 pilus no such difference appears. The reason for the latter can be attributed to the force-modulating property of the pilus, which temporarily regulates the force to the same value, ~120 pN, irrespective of the actual load. Also, for both tethers, the time needed to reach the STD was affected by the use of the correction coefficients. The influence of these coefficients will presumably be of importance when simulating processes such as the rolling behavior of cells that have multiple bonds interacting with a surface.

Most adhesive biological processes are exposed to mechanical stress from fluid-induced shear in dynamic environments. Handling this stress is important both for bacteria initially attaching to host tissue and for those that already have colonized. For this purpose uropathogenic bacteria have developed helixlike surface organelles as sophisticated

mediators of attachment. It has been demonstrated that such bacteria cannot adhere in the absence of pili (6). The same is valid for bacteria in other environments. For example, a hemagglutination assay showed that colonization-factor-antigen I expressed by enterotoxigenic *E. coli* bacteria exposed to shear flow did not stay bound when the helical region of the pilus was mutated into an open coiled stalk (42). In addition, a force spectroscopy study illustrated that colonization-factor-antigen I pili show uncoiling abilities similar to those of type 1 pili (43). All this implies that the helixlike structure of pili is important in the adhesion process for many bacteria. Moreover, that the attachment organelles always act jointly with the adhesin bond supports the assumption previously proposed by Forero et al. (11) that they have coevolved to reinforce their total influence on the survival probability of the bacterium. The study presented here, which demonstrates that the ability of the type 1 pilus shaft to regulate forces from hundreds of pN to 120 pN coincides with the specific properties of the FimH adhesin-receptor bond, thus demonstrates that the assumption that the pili and the adhesin have coevolved is reasonable.

SUPPORTING MATERIAL

Five figures, one, table, methods, and one movie are available at http://www.biophysj.org/biophysj/supplemental/S0006-3495(13)00443-8.

This work was performed within the Umeå Centre for Microbial Research (UCMR) Linnaeus Program with support from Umeå University and the Swedish Research Council (349-2007-8673). It was also supported by a Young Researcher Award (Karriärbidrag) from Umeå University to M.A. and by a grant from the Swedish Research Council (621-2008-3280) to O.A.

REFERENCES

1. Vogel, A., B. Elmabsout, and D. Gintz. 2004. Modélisation du champ des vitesses de l'urine dans un bolus urétéral. *C. R. Mec.* 332: 737–742.
2. Kim, J., P. Moin, and R. Moser. 1987. Turbulence statistics in fully developed channel flow at low Reynolds number. *J. Fluid Mech.* 177:133–166.
3. Lenaers, P., Q. Li, …, R. Orlu. 2012. Rare backflow and extreme wall-normal velocity fluctuations in near-wall turbulence. *Phys. Fluids.* 24:035110.
4. Jin, Q., X. Zhang, …, J. Wang. 2010. Dynamics analysis of bladder-urethra system based on CFD. *Front. Mech. Eng. China.* 5:336–340.
5. Abrams, P. 1997. Urodynamics. Springer - Verlag, London.
6. Mulvey, M. A. 2002. Adhesion and entry of uropathogenic *Escherichia coli*. *Cell. Microbiol.* 4:257–271.
7. Johnson, J. R. 1991. Virulence factors in *Escherichia coli* urinary tract infection. *Clin. Microbiol. Rev.* 4:80–128.
8. Melican, K., R. M. Sandoval, …, A. Richter-Dahlfors. 2011. Uropathogenic *Escherichia coli* P and Type 1 fimbriae act in synergy in a living host to facilitate renal colonization leading to nephron obstruction. *PLoS Pathog.* 7:e1001298.
9. Thomas, W. E., E. Trintchina, …, E. V. Sokurenko. 2002. Bacterial adhesion to target cells enhanced by shear force. *Cell.* 109:913–923.
10. Thomas, W. E., L. M. Nilsson, …, V. Vogel. 2004. Shear-dependent 'stick-and-roll' adhesion of type 1 fimbriated *Escherichia coli*. *Mol. Microbiol.* 53:1545–1557.
11. Forero, M., O. Yakovenko, …, V. Vogel. 2006. Uncoiling mechanics of *Escherichia coli* type I fimbriae are optimized for catch bonds. *PLoS Biol.* 4:e298.
12. Hahn, E., P. Wild, …, S. A. Müller. 2002. Exploring the 3D molecular architecture of *Escherichia coli* type 1 pili. *J. Mol. Biol.* 323: 845–857.
13. Bullitt, E., and L. Makowski. 1998. Bacterial adhesion pili are heterologous assemblies of similar subunits. *Biophys. J.* 74:623–632.
14. Fällman, E., S. Schedin, …, O. Axner. 2005. The unfolding of the P pili quaternary structure by stretching is reversible, not plastic. *EMBO Rep.* 6:52–56.
15. Andersson, M., E. Fällman, …, O. Axner. 2006. Dynamic force spectroscopy of *E. coli* P pili. *Biophys. J.* 91:2717–2725.
16. Andersson, M., B. E. Uhlin, and E. Fällman. 2007. The biomechanical properties of *E. coli* pili for urinary tract attachment reflect the host environment. *Biophys. J.* 93:3008–3014.
17. Castelain, M., A. E. Sjöström, …, M. Andersson. 2010. Unfolding and refolding properties of S pili on extraintestinal pathogenic *Escherichia coli*. *Eur. Biophys. J.* 39:1105–1115.
18. Castelain, M., S. Ehlers, …, O. Axner. 2011. Fast uncoiling kinetics of F1C pili expressed by uropathogenic *Escherichia coli* are revealed on a single pilus level using force-measuring optical tweezers. *Eur. Biophys. J.* 40:305–316.
19. Chen, F.-J., C.-H. Chan, …, L. Hsu. 2011. Structural and mechanical properties of *Klebsiella pneumoniae* type 3 Fimbriae. *J. Bacteriol.* 193:1718–1725.
20. Andersson, M., E. Fällman, …, O. Axner. 2006. Force measuring optical tweezers system for long time measurements of P pili stability. *Proc. SPIE.* 6088:286–295.
21. Björnham, O., O. Axner, and M. Andersson. 2008. Modeling of the elongation and retraction of *Escherichia coli* P pili under strain by Monte Carlo simulations. *Eur. Biophys. J.* 37:381–391.
22. Thomas, W. E., M. Forero, …, V. Vogel. 2006. Catch-bond model derived from allostery explains force-activated bacterial adhesion. *Biophys. J.* 90:753–764.
23. Whitfield, M., T. Ghose, and W. E. Thomas. 2010. Shear-stabilized rolling behavior of *E. coli* examined with simulations. *Biophys. J.* 99:2470–2478.
24. Zakrisson, J., K. Wiklund, …, M. Andersson. 2012. Helix-like biopolymers can act as dampers of force for bacteria in flows. *Eur. Biophys. J.* 41:551–560.
25. Andersson, M., E. Fällman, …, O. Axner. 2006. A sticky chain model of the elongation and unfolding of *Escherichia coli* P pili under stress. *Biophys. J.* 90:1521–1534.
26. Kinn, A. C. 1996. Progress in urodynamic research on the upper urinary tract: implications for practical urology. *Urol. Res.* 24:1–7.
27. Jeffrey, B., H. S. Udaykumar, and K. S. Schulze. 2003. Flow fields generated by peristaltic reflex in isolated guinea pig ileum: impact of contraction depth and shoulders. *Am. J. Physiol. Gastrointest. Liver Physiol.* 285:G907–G918.
28. Vahidi, B., N. Fatouraee, …, A. N. Moghadam. 2011. A mathematical simulation of the ureter: effects of the model parameters on ureteral pressure/flow relations. *J. Biomech. Eng.* 133:031004.
29. Smith, C. R., J. D. a. Walker, …, U. Sobrun. 1991. On the dynamics of near-wall turbulence. *Philos. Transact. A Math. Phys. Eng. Sci.* 336:131–175.
30. Xu, C., Z. Zhang, …, F. T. M. Nieuwstadt. 1996. Origin of high kurtosis levels in the viscous sublayer. Direct numerical simulation and experiment. *Phys. Fluids.* 8:1938–1944.
31. Yakovenko, O., S. Sharma, …, W. E. Thomas. 2008. FimH forms catch bonds that are enhanced by mechanical force due to allosteric regulation. *J. Biol. Chem.* 283:11596–11605.

32. Marchioli, C., and A. Soldati. 2002. Mechanisms for particle transfer and segregation in a turbulent boundary layer. *J. Fluid Mech.* 468:283–315.

33. Goldman, A., and R. G. Cox. 1967. Slow viscous motion of a sphere parallel to a plane wall. *Chem. Eng. Sci.* 22:653–660.

34. Happel, J., and H. Brenner. 1983. Low Reynolds Number Hydrodynamics. Kluwer Academic, Dordrecht, The Netherlands.

35. Saffman, P. G. 1968. Correction. *J. Fluid Mech.* 31:624.

36. Saffman, P. G. 1965. The lift on a small sphere in a slow shear flow. *J. Fluid Mech.* 22:385–400.

37. Cherukat, P., and J. B. McLaughlin. 1994. The inertial lift on a rigid sphere in a linear shear-flow field near a flat wall. *J. Fluid Mech.* 263:1–18.

38. Brenner, H. 1961. The slow motion of a sphere through a viscous fluid towards a plane surface. *Chem. Eng. Sci.* 16:242–251.

39. Schäffer, E., S. F. Nørrelykke, and J. Howard. 2007. Surface forces and drag coefficients of microspheres near a plane surface measured with optical tweezers. *Langmuir.* 23:3654–3665.

40. Bell, G. I. 1978. Models for the specific adhesion of cells to cells. *Science.* 200:618–627.

41. Andersson, M., O. Axner, …, E. Fällman. 2008. Physical properties of biopolymers assessed by optical tweezers: analysis of folding and refolding of bacterial pili. *ChemPhysChem.* 9:221–235.

42. Li, Y.-F., S. Poole, …, E. Bullitt. 2009. Structure of CFA/I fimbriae from enterotoxigenic *Escherichia coli*. *Proc. Natl. Acad. Sci. USA.* 106:10793–10798.

43. Andersson, M., O. Björnham, …, E. Bullitt. 2012. A structural basis for sustained bacterial adhesion: biomechanical properties of CFA/I pili. *J. Mol. Biol.* 415:918–928.